

X-ray photoelectron spectroscopy study of mixed-valence effects and charge fluctuation in $\text{Na}_x\text{V}_2\text{O}_5$

M. J. Konstantinović and S. Van den Berghe

SCK-CEN, Studiecentrum voor Kernenergie/Centre d'Etude de l'Energie Nucléaire, Boeretang 200, B-2400 Mol, Belgium

M. Isobe and Y. Ueda

Institute for Solid State Physics, The University of Tokyo, 5-11-5 Kashiwanoha, Kashiwa, Chiba 277-8581, Japan

(Received 18 April 2005; revised manuscript received 6 July 2005; published 28 September 2005)

X-ray photoelectron spectra of vanadium $2p$ states in α' - NaV_2O_5 and γ - LiV_2O_5 , single crystals show distinct splitting of both $j=1/2$ and $j=3/2$ spin-orbit lines due to the existence of V^{4+} and V^{5+} ions. In contrast to γ - LiV_2O_5 , the α' - NaV_2O_5 exhibits the disproportional intensities and larger binding energy difference of $(\text{V}^{4+})2p^{3/2}$ and $(\text{V}^{5+})2p^{3/2}$ lines, that we attribute to a charge delocalization effect. By increasing the sodium deficiency, both effects reduce in a very good agreement with a model that takes into account the relative abundance of V^{4+} and V^{5+} ions, and the change of degree of delocalization. We estimate that sodium deficiency of about 15% increases electron localization by about 0.4%.

DOI: [10.1103/PhysRevB.72.125124](https://doi.org/10.1103/PhysRevB.72.125124)

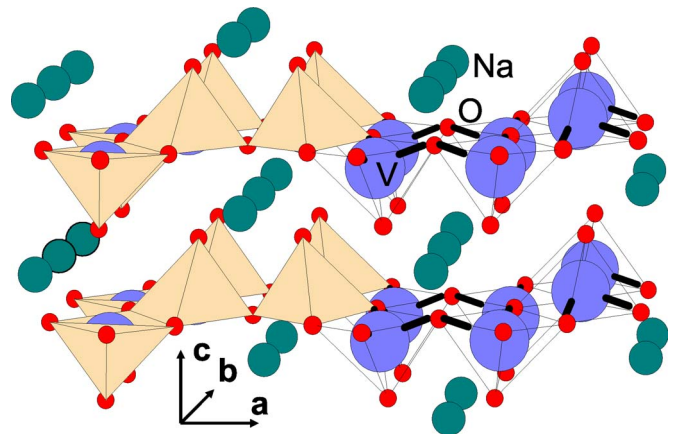
PACS number(s): 79.60.-i, 71.30+h, 75.50.Ee, 75.30.Mb

I. INTRODUCTION

α' - NaV_2O_5 belongs to the vanadate family of transition metal oxides which exhibits various effects originating from strong electron correlations.^{1,2} The structure of α' - NaV_2O_5 , as well as other members of the family represented with a general chemical formula AV_2O_5 , consists of vanadium-oxygen pyramids (VO_5) that are connected via common edges and corners to form layers in the **ab** plane, see Fig. 1. Its structure can be described as an array of parallel ladders running along the **b** axis, where each rung is made of a V-O-V bond. The A elements are situated between layers as intercalants, but in fact they determine the valence state of the vanadium atoms acting as charge reservoirs. If $A=\text{Na}$, Li the single electron is donated to each rung, the formal valence state of vanadium is $\text{V}^{4.5+}$, and there are equal numbers of V^{4+} and V^{5+} ions in the unit cell. In the case where the A place is filled by an alkaline earth metal, for example by Ca or Mg ions, the V-O-V rung contains two electrons and all vanadium atoms are in the V^{4+} state. Interestingly, the mixed valence at room temperature produces quite different ground states in γ - LiV_2O_5 and α' - NaV_2O_5 . While the crystal structure of γ - LiV_2O_5 is in full agreement with the existence of two different V^{4+} and V^{5+} states, the high-temperature (HT) phase of α' - NaV_2O_5 requires that all vanadium atoms are indistinguishable in the unit cell as they all have an average valence of $\text{V}^{4.5+}$. This symmetry equivalence is clearly demonstrated with x-ray diffraction (XRD),³ and by infrared (IR) and Raman spectroscopies.⁴ Moreover, the HT charge-disordered phase of α' - NaV_2O_5 is not stable and the crystal undergoes a phase transformation² at $T_c=34$ K into a zig-zag (along the **b** axis) charge ordered (CO) phase with two different V^{4+} and V^{5+} positions.⁵ The exact CO pattern has been recently unambiguously determined by resonant x-ray scattering.⁶ In contrast to vanadium oxygen compounds without the A type of intercalants which exhibit Mott metal-insulator type of phase transitions, such as V_2O_3 , VO_2 , and

$\text{V}_{2n}\text{O}_{5n-2}$ (V_6O_{13} is also a mixed valence compound),¹ both HT and LT phases of α' - NaV_2O_5 have strong insulating character with a charge gap of about 1 eV.⁷ The insulating properties of the HT ground state in α' - NaV_2O_5 can be associated with the splitting of the V- d_{xy} band due to electron correlations, or/and to the combined effects of short range Coulomb interaction and charge disproportionation along the rung within t - j -V type of models.^{5,9,10} However, the temperature behavior of the charge gap, presumably represented by the feature in the optical conductivity at about 1 eV, shows no anomaly at T_c , and is in disagreement with theoretical predictions.⁷ In addition, similar optical transitions are found in the optical conductivity spectra of γ - LiV_2O_5 , which exhibits no charge fluctuations, and it is in some form of CO state already at room temperature.⁸

Thus, one may equally regard the spin-gap, which opens below the critical temperature, as the order parameter. Namely, the CO phase transition in α' - NaV_2O_5 can be also analyzed from the magnetism point of view. The HT phase exhibits a one-dimensional antiferromagnetic (1D AF) order-

FIG. 1. (Color online) Crystal structure of α' - NaV_2O_5 .

ing along the **b** axis due to a small superexchange interaction (bond angle close to 90°) between neighboring ladders. Then, the phase transition at 34 K could, in principle, be of the spin-Peierls (SP) type characterized by a transformation of an 1D AF into a nonmagnetic spin-singlet state with a nonzero spin gap.² This route was abandoned shortly after initial proposal,² since the critical temperature is found to be insensitive to the applied magnetic field.

Additional arguments, pointing to the non adequacy of the current description of the electronic structure and phase transition in α' - NaV_2O_5 , came from the effects related to sodium deficiency. Sodium deficiency changes the relative abundance of the V^{4+} and V^{5+} ions, i.e., introduces holes in the system leading to the formation of rungs without electrons similar to the $\text{V}^{5+}\text{-O}_3\text{-V}^{5+}$ bonds in V_2O_5 . The hole doping is expected to drive the Fermi level into the $\text{V-}d_{xy}$ bonding band,⁷ causing the appearance of a metallic state in α' - $\text{Na}_x\text{V}_2\text{O}_5$. This is not confirmed experimentally. The persistence of “strong” insulating behavior, in spite of large deficiency in α' - $\text{Na}_x\text{V}_2\text{O}_5$, is evident from the IR spectra and ellipsometry measurements,¹² as well as from the transport measurements.² Moreover, by increasing the sodium deficiency, the absorption peak at 0.9 eV shifts towards higher energies indicating that this excitation might have a polaron character.¹³ Thus, in spite of accumulated experimental evidence, the lattice effects have not been taken into consideration until very recently,¹⁴ as a possible driving mechanism of the phase transition in α' - NaV_2O_5 . The second experimental fact that has been completely ignored is the electron interaction along the **c** axis, in spite of clearly demonstrated significance through the observation of a “devils staircase” type phase transition under high pressure.¹⁵

Therefore, we are still confronted with a question: How do we experimentally probe the correlation effects in α' - NaV_2O_5 , and what would the proper order parameter of the CO phase transition at 34 K be?

Here we investigate the charge delocalization in α' - $\text{Na}_x\text{V}_2\text{O}_5$ by x-ray photoelectron spectroscopy (XPS). We analyze the $\text{V}2p$ core level spectra of nominally pure and sodium deficient α' - $\text{Na}_x\text{V}_2\text{O}_5$, and we discuss the interplay between effects related to the charge localization-delocalization process and those appearing due to the change of the relative abundance of V^{4+} and V^{5+} ions. From a comparison between measured and calculated values of the intensity ratio and binding energy difference between $(\text{V}^{4+})2p^{3/2}$ and $(\text{V}^{5+})2p^{3/2}$ lines, we determine the degree of charge delocalization and its relationship to the sodium deficiency in α' - $\text{Na}_x\text{V}_2\text{O}_5$.

II. EXPERIMENT

This work was performed on single crystal plates of α' - $\text{Na}_x\text{V}_2\text{O}_5$ ($0.85 \leq x \leq 1.00$) with dimensions typically about $2 \times 4 \times 0.5 \text{ mm}^3$ in the **a**, **b**, and **c** axes, respectively, single crystal of $\gamma\text{-LiV}_2\text{O}_5$ ($2 \times 3 \times 1 \text{ mm}^3$), and high-quality single-phase polycrystalline CaV_2O_5 . The details of the sample preparation were published elsewhere.^{2,11} The crystals were freshly cleaved *ex situ* parallel to the **ab** plane and gave mirrorlike surfaces. The measurements were taken from

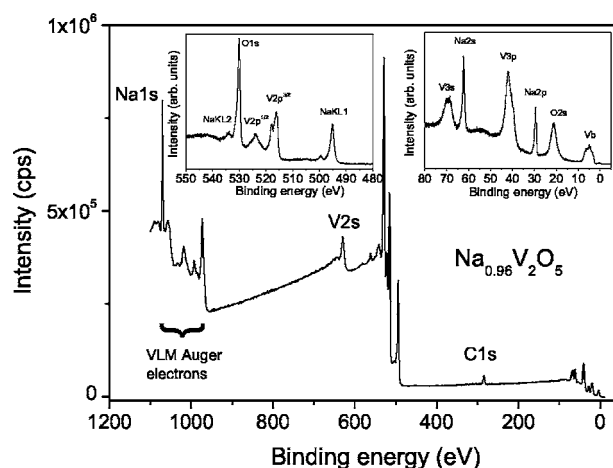


FIG. 2. XPS spectra of $\text{Na}_{0.96}\text{V}_2\text{O}_5$ single crystal measured with a monochromatic $\text{Al } K\alpha$ radiation.

several cleaved surfaces to confirm reproducibility. The XPS measurements were done with an Escalab 250 spectrometer, that provides a monochromatic $\text{Al } K\alpha$ radiation with a spot size in the range of 0.1 to 1 mm (typically $\sim 500 \mu\text{m}$), and a hemispherical analyzer with a maximal energy resolution of 0.018 eV. The base pressure was better than 1×10^{-10} mbar. The fit of the XPS spectra is done with the Avantage Data Spectrum Processing Package (Thermo VG Scientific).

III. MIXED VALENCE EFFECTS IN XPS SPECTRA

A typical XPS spectrum of α' - $\text{Na}_x\text{V}_2\text{O}_5$ single crystals is shown in Fig. 2. In addition to a weak carbon $\text{C}1s$ line (indicates low contamination), which is found in most samples in spite of fresh cleavage, we observed peaks that correspond to the core level excitations of Na, V, and O ions in the spectra. The lines at binding energies below 10 eV originate from valence band electrons, and are denoted as V_b . No charging effects are observed and the energy variation of the $\text{C}1s$ lines in different spectra is found to be within 0.05 eV. The spin-orbit coupling (L - S) splits the vanadium $\text{V}2p$ and $\text{V}3p$ states into two $j=1/2$ and $j=3/2$ states, by ~ 8 and ~ 2 eV, respectively, see inset Fig. 2. In addition to L - S splitting, we observed additional features in the spectra close to the $\text{V}2p$ lines, so we focus our attention to the energy region around 520 eV.

In Fig. 3 we present the XPS spectra in the 510–530 eV range for three different compounds: α' - NaV_2O_5 , $\gamma\text{-LiV}_2\text{O}_5$, and CaV_2O_5 . The spectra are obtained in high resolution mode, with 5 eV pass energy, and presented without any corrections. The best fit of the XPS spectra for α' - NaV_2O_5 and $\gamma\text{-LiV}_2\text{O}_5$ is obtained by including six peaks in the fit on a Shirley background. The fit is also shown in Fig. 3, and the parameters are collected in Table I. The peak labeled C at about 517.6 eV in α' - NaV_2O_5 is also observed in $\gamma\text{-LiV}_2\text{O}_5$ but not in CaV_2O_5 . Since there are only V^{4+} ions in CaV_2O_5 , we assign this line to an excitation from the $(\text{V}^{5+})2p^{3/2}$ state. Following the same line of reasoning, we assign the A peak at about 515.6 eV in α' - NaV_2O_5

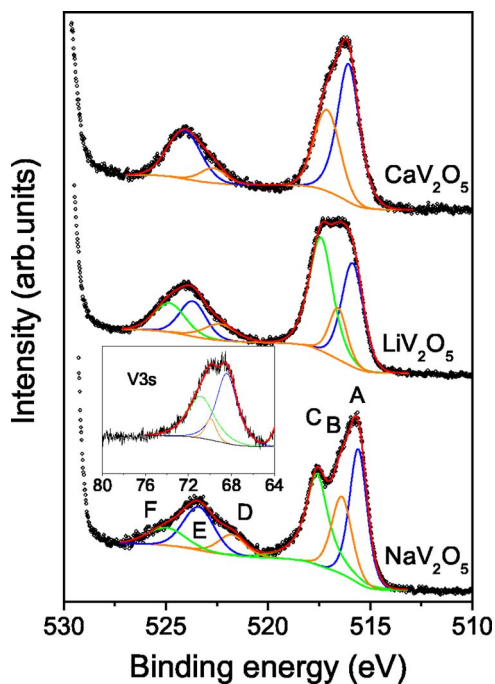


FIG. 3. (Color online) XPS spectra of $V2p$ core level electrons in α' - NaV_2O_5 , γ - LiV_2O_5 , and CaV_2O_5 . The circles are experimental data, and the fits are represented with solid lines. Inset: XPS spectra of $V3s$ core level electrons

(515.9 eV in γ - LiV_2O_5 and 516.1 eV in CaV_2O_5) to the excitations of the $(V^{4+})2p^{3/2}$ state. The binding energies are in good agreement with previous measurements.¹⁶ The appearance of the third feature (B) at an energy of about 516.3 eV is attributed to a final state exchange splitting effect (similar three-peak structure is also found in the case of $V3s$ level, see Inset Fig. 3). Namely, such core level splitting can occur when the ion has unpaired electrons in the valence band. As we already discussed, the vanadium V^{4+} ion has one unpaired electron in the $3d$ state. After ejection of the $V2p$ electron by x rays, one additional unpaired electron is present, which can interact with the electron in the valence band via exchange. The spins of these two electrons can couple either ferromagnetically (parallel spins), or antiferromagnetically (antiparallel), which results in two states with different energies. The splitting is measured to be in the range of 0.8 to 1 eV for all three compounds, see Table I. The intensity ratio is found to be in the range of 1.6 to 2, while simple theoretical prediction gives $I_{\uparrow\uparrow}/I_{\uparrow\downarrow}=(S+1)/S=3$ (the $S=1/2$ is the total spin of the unpaired electrons in the valence band). The exchange splitting is not found for $(V^{5+})2p^{3/2}$ state, see Fig. 3, which is in excellent agreement with the fact that the exchange splitting is absent in the V^{5+} ion, since there is no unpaired electron in the $3d$ state. The final state exchange splitting effect is already observed^{17,18} and analyzed in VO_2 (consists of V^{4+} ions), which gives additional arguments in favor of our assignment. Similar conclusions can be drawn for the $V2p^{1/2}$ state. The binding energy differences in α' - NaV_2O_5 are $E_{\text{BE}}^F-E_{\text{BE}}^C=7.35$ eV, and $E_{\text{BE}}^E-E_{\text{BE}}^A=7.8$ eV. Similarly, in γ - LiV_2O_5 we find $E_{\text{BE}}^F-E_{\text{BE}}^C=7.45$ eV, and $E_{\text{BE}}^E-E_{\text{BE}}^A=7.76$ eV, so we assign the E and F

TABLE I. Fit parameters.

NaV_2O_5	BE (eV)	Height (cps)	Height ratio	Area (cps)	Area ratio	FWHM (eV)
A	515.58	1564	1.00	1769	0.96	1.06
B	516.39	906.1	0.58	1163	0.63	1.21
C	517.62	1063	0.68	1834	1.00	1.31
D	521.77	238.8	0.15	409.3	0.22	1.62
E	523.38	503.3	0.34	963	0.52	1.84
F	524.97	204.5	0.13	480.8	0.26	2.26
LiV_2O_5	BE (eV)	Height (cps)	Height ratio	Area (cps)	Area ratio	FWHM (eV)
A	515.86	960	0.92	1332	0.82	1.32
B	516.57	475	0.45	538.4	0.33	1.07
C	517.41	1048	1.00	1634	1.00	1.42
D	522.36	150.5	0.14	309.4	0.18	1.92
E	523.68	336.4	0.31	534.7	0.32	1.57
F	524.82	269.4	0.26	532.2	0.32	1.88
CaV_2O_5	BE (eV)	Height (cps)	Height ratio	Area (cps)	Area ratio	FWHM (eV)
A	516.06	443.8	1.00	647.2	1.00	1.33
B	517.11	261.7	0.59	419.2	0.65	1.54
D	522.68	47.84	0.11	77.06	0.12	1.54
E	524.10	154.7	0.35	317.4	0.49	1.96

peaks to the the excitations of the $(V^{4+})2p^{1/2}$ and $(V^{5+})2p^{1/2}$ states, respectively. Finally, the D peak corresponds to the exchange splitting of $(V^{4+})2p^{1/2}$ state.

Interestingly, we found the intensity ratio of $(V^{5+})2p^{3/2}$ and $(V^{4+})2p^{3/2}$ peaks to be considerably different in α' - NaV_2O_5 and γ - LiV_2O_5 , see Fig. 3 and Table I. It is, in fact, more appropriate for such analyzes to consider the integrated intensities, so in the rest of the paper we will use the ratio of the areas under the peaks. The A and B peaks originate from the exchange splitting of the $V2p$ state of the V^{4+} ion, thus, as the proper intensity ratio of $(V^{5+})2p^{3/2}$ and $(V^{4+})2p^{3/2}$ lines, we take I_C/I_{A+B} . In γ - LiV_2O_5 this ratio is close to 1, which is a consequence of the fact that there are equal numbers of V^{4+} and V^{5+} ions in the unit cell. On the other hand, $I_C/I_{A+B} \sim 0.63$ in α' - NaV_2O_5 . Since there is no inequality in α' - NaV_2O_5 in that respect, we attribute the strong peak disproportion to the charge delocalization effect. As we already mentioned, the electron interaction between V^{4+} and V^{5+} ions is sufficiently large to cause the charge delocalization and symmetrical ground state in α' - NaV_2O_5 , which manifests through the disproportional line intensities in the XPS spectra. According to the Hush model¹⁹ the intensities are found to be quite sensitive to a small departure from electron localization, and in the mixed valence case with two formal oxidation states, the intensity ratio can be related to

$$\frac{I_{V^{5+}}}{I_{V^{4+}}} = f_{\text{corr}} = \left(\frac{1 + \sqrt{1 + \frac{4J^2}{\Delta E^2}} - \frac{4J}{\Delta E}}{1 + \sqrt{1 + \frac{4J^2}{\Delta E^2}} + \frac{4J}{\Delta E}} \right)^2, \quad (1)$$

where J is the electronic coupling integral between V^{4+} and V^{5+} states, and ΔE is the binding energy difference at $J=0$, $\Delta E = E_{\text{BE}}[(V^{4+})2p^{3/2}] - E_{\text{BE}}[(V^{5+})2p^{3/2}]$. At $J \neq 0$ the binding energy difference increases, i.e., the peaks move further apart from each other, which is also observed in our spectra. Namely, in α' - NaV_2O_5 we find $\Delta E_{\text{NaV}_2\text{O}_5} = E_C - E_A = 2.04$ eV, while in γ - LiV_2O_5 $\Delta E_{\text{LiV}_2\text{O}_5} = E_C - E_A = 1.43$ eV. Such additional splitting of the binding energy due to charge delocalization¹⁹ is

$$\Delta E_{\text{corr}} = \Delta E \left(\sqrt{1 + \frac{4J^2}{\Delta E^2}} - 1 \right). \quad (2)$$

Equation (1) reproduces well the intensity disproportion by taking $\Delta E = 2$ eV and $J = 0.23$ eV. These parameters are in agreement with the experimental binding energy difference $\Delta E_{\text{NaV}_2\text{O}_5} = 2.04$ eV. As we see from this analysis, and we will discuss it in more detail below, the difference in splitting between α' - NaV_2O_5 and γ - LiV_2O_5 of about 0.61 eV is too large to be entirely the result of electron delocalization, since $\Delta E_{\text{corr}} = 0.04$ eV. In addition, the value of the electronic coupling integral $J = 0.23$ eV is also somewhat larger than the estimated value, of about 0.07 eV, from the susceptibility measurements (the maximum of the susceptibility curve is at about 350–400 K). We mention at least two important contributions that could cause this discrepancy. A first effect is related to the Madelung energy, which is completely ignored in the Hush model in spite of theoretical models of the charge ordering phase transition in NaV_2O_5 which indicate its importance.²⁰ Second effect is related to the exchange splitting. Namely as an experimental binding energy difference we consider $\Delta E_{\text{NaV}_2\text{O}_5} = E_A - E_C = 2.04$ eV which is not entirely correct since we ignore the exchange splitting. It seems more appropriate to consider the first moment of the spectrum, but due to the complexity of the final state effect, its correctness would be very difficult to estimate. Nevertheless, both effects would lower ΔE and consequently J .

The XPS spectra of sodium deficient samples α' - $\text{Na}_x\text{V}_2\text{O}_5$ are shown in Fig. 4. The spectra are normalized by using the $\text{O}1s$ line intensity. The results of the fit, e.g., the relative intensity ratios and the binding energy differences as a function of the sodium deficiency are summarized in Fig. 5. By reducing the sodium content, the relative intensity ratio between $(V^{5+})2p^{3/2}$ and $(V^{4+})2p^{3/2}$ peaks changes in favor of the $(V^{5+})2p^{3/2}$ peak. This is expected since the relative abundance of V^{4+} and V^{5+} ions changes. The XPS intensity is directly proportional to the ion concentration, so the intensity ratio due to sodium deficiency should be proportional to $1/x$, where x is Na concentration. For example, $x=0.5$ corresponds to the situation where there are twice as many V^{5+} ions in the unit cell than V^{4+} ions. Therefore, by putting together the correlation term and the term related to the

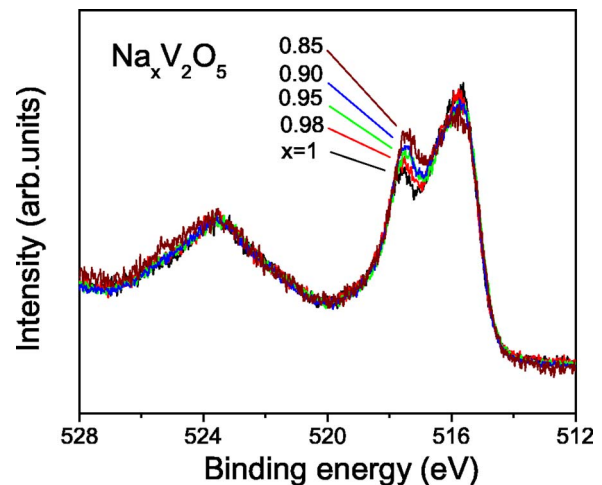


FIG. 4. (Color online) XPS spectra of $V2p$ core level electrons in α' - NaV_2O_5 , with $x=1, 0.98, 0.95, 0.90$, and 0.85 .

change of the relative abundance of V^{4+} and V^{5+} ions, we obtain the following equation:

$$\frac{I_{V^{5+}}}{I_{V^{4+}}} = \frac{1}{x} f_{\text{corr}}. \quad (3)$$

The result of the calculation, assuming the same values of the parameters as above ($\Delta E = 2$ eV and $J = 0.23$ eV.), is presented with a dashed line in Fig. 5(a). For $x=1$, the $I_{V^{5+}}/I_{V^{4+}} = 0.63$, and the intensity ratio is entirely governed by electron delocalization. By increasing x , the delocalization effect is compensated due to the appearance of a dis-equilibrium between the number of V^{4+} and V^{5+} ions. At x

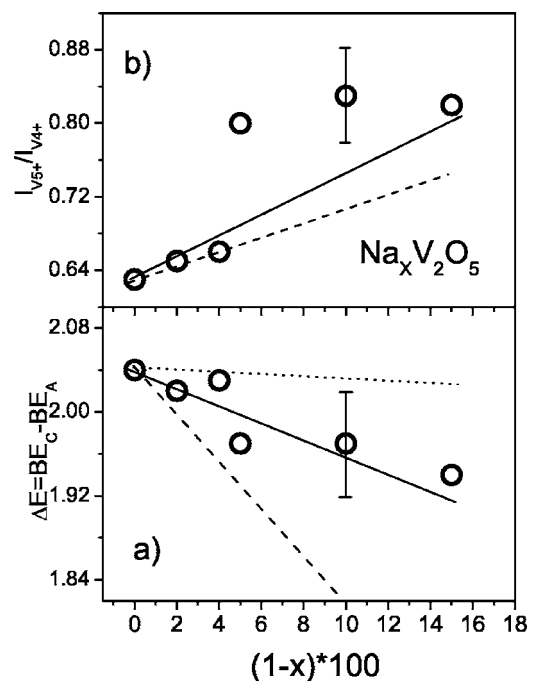


FIG. 5. Binding energy difference and intensity ratio of $(V^{5+})2p^{3/2}$ and $(V^{4+})2p^{3/2}$ lines as a function of sodium deficiency.

$=0.85$, which is the maximal doping concentration experimentally achieved, the calculation gives $I_{V^{5+}}/I_{V^{4+}}=0.74$. This value is considerably smaller than the measured value, see Fig. 5(a). In another words, the compensation effect seems to be more pronounced than one described by Eq. (3). This is not entirely unexpected since, by diluting the system, we effectively change the interaction between V^{4+} and V^{5+} ions. By increasing the sodium deficiency, J should decrease, and we assume a linear dependence $J_{\text{eff}}=Jx$ in our calculation. The linear dependence can be justified by the following reasoning: The exchange integral is, in the first approximation, inversely proportional to the distance between ions, denoted as r . At $x=0.5$ every second V^{4+} ion is replaced by V^{5+} ion and the average distance between V^{4+} and V^{5+} is $2r$. The result that takes this correction into account is presented with a full line in Fig. 5(a). We obtain a much better agreement with experiment, which clearly demonstrates that sodium deficiency reduces the charge delocalization effect. Our finding can be nicely related to the observations^{22,23} that sodium deficiency destroys the low temperature charge ordered state. Namely, the low temperature CO state is almost fully suppressed at sodium deficiencies larger than 3%.

The analysis of the electron delocalization effect on the basis of binding energies is much more difficult to perform. There are two main reasons: First, even though we limit our discussion to the binding energy difference, which eliminates the effects related to the shift of the Fermi level, or surface effects for example, it is practically impossible to accurately control all relevant parameters that are determining the binding energies. Second, the binding energy difference is, according to the Hush model,¹⁹ much less sensitive to the electron delocalization effect than the intensity ratio. Nevertheless, let us start by completely ignoring the electron delocalization effects, and analyze what should be the effect of sodium deficiency on the binding energy difference on the basis of chemical shifts. By increasing the sodium deficiency, the effective valence electron density decreases. For example, the largest deficiency at $x=0.85$ gives about +4.575 average valence for the vanadium ions. If we ignore the Madelung energy, the charge potential model²¹ predicts an increase of the binding energy due to a decrease in valence electron density. Therefore, the center of gravity between two $V2p^{3/2}$ peaks should move towards higher binding energies. It is reasonable to expect that such a shift would occur mainly through the shift of $(V^{4+})2p$ line, since in the hypothetical situation with very small sodium content, the XPS spectra should approach the V_2O_5 case (only V^{5+} ions). Thus, the binding energy difference ΔE should scale with x or, more precisely, should decrease by increasing the sodium deficiency. The change of the binding energy difference we describe as

$$\Delta E_{\text{charge}} = k\Delta Q = \Delta E(1-x), \quad (4)$$

which in combination with the correlation term gives

$$\Delta E' = \Delta E - \Delta E_{\text{charge}} + \Delta E_{\text{corr}}. \quad (5)$$

For $\Delta E_{\text{corr}}=0$ these equations ensure that in the limit of $x=0$ the $(V^{4+})2p$ and $(V^{5+})2p$ peaks overlap. This case is represented by the dashed line in Fig. 5(b). We immediately see that the calculation overestimates the change in binding energy. In the same graph we present by the dotted line the change of the binding energy difference in the case where the correlation effect is taken into account (we take the same parameters as for the intensity ratio considerations, $\Delta E=2$ eV, $J=0.23x$), without taking into account the chemical shift effect, $\Delta E_{\text{charge}}=0$. In this limit the effect is, however, underestimated. By combining the two effects the agreement with experiment is getting worse, since the shift due to the change of the exchange integral would simply add to the chemical shift. Therefore, the main source of disagreement is the scaling behavior of the chemical shift represented by Eq. (4). Introduction of the Madelung energy term, which requires more elaborate theoretical analysis, might help to improve agreement with experiment, and enable extraction of the electron delocalization effect from the binding energy data. At this point we just note that a good agreement with experimental data can be obtained by taking the chemical shift in the form $\Delta E_{\text{charge}}=\Delta E/2(1-x)$, which is represented with a full line in Fig. 5(b).

Finally, we estimate the magnitude of the electron delocalization from electron probability functions¹⁹

$$\rho_a = \frac{\frac{4J^2}{\Delta E^2}}{2\left(1 + \sqrt{1 + \frac{4J^2}{\Delta E^2} + \frac{4J^2}{\Delta E^2}}\right)}, \quad (6)$$

$$\rho_b^2 = 1 - \rho_a^2. \quad (7)$$

Using the same values of parameters $\Delta E=2$ eV and $J=0.23x$, we obtain that for $x=1$ the valence electron is 99% localized at V^{4+} site. The sodium deficiency decreases the electron delocalization, so at $x=0.85$ the localization is about 99.4%.

IV. CONCLUSION

We study the charge fluctuation and mixed valence effects in α' - $\text{Na}_x\text{V}_2\text{O}_5$ single crystals by using x-ray photoelectron spectroscopy. We measure the intensity ratio and the binding energy difference of $(V^{4+})2p^{3/2}$ and $(V^{5+})2p^{3/2}$ lines as a function of sodium deficiency, and compare them to the observations in γ - LiV_2O_5 and CaV_2O_5 . In nominally pure α' - NaV_2O_5 the intensities of these two lines are found to be disproportional, while in γ - LiV_2O_5 the intensity ratio is close to 1. Moreover, their binding energy difference is larger than in the case of γ - LiV_2O_5 . We attribute these two effects to charge delocalization. By increasing the sodium deficiency, both effects reduce in very good agreement with a model that takes into account the relative abundance of V^{4+} and V^{5+} ions, and the change of degree of delocalization. We estimate that a sodium deficiency of about 15% increases electron localization by about 0.4%.

- ¹M. Imada, A. Fujimori, and Y. Tokura, *Rev. Mod. Phys.* **70**, 1039 (1998).
- ²M. Isobe and Y. Ueda, *J. Phys. Soc. Jpn.* **65**, 1178 (1996).
- ³H-G von Schnering, Yu. Grin, M. Kaupp, M. Somer, R. Kremer, O. Jepsen, T. Chatterji, and M. Weiden, *Z. Kristallogr.* **246**, 213 (1998).
- ⁴Z. V. Popović, M. J. Konstantinović, R. Gajić, V. Popov, Y. S. Raptis, A. N. Vasil'ev, M. Isobe, and Y. Ueda, *J. Phys.: Condens. Matter* **10**, L513 (1998).
- ⁵H. Seo and H. Fukujama, *J. Phys. Soc. Jpn.* **67**, 2602 (1998).
- ⁶K. Ohwada, Y. Fujii, Y. Katsuki, J. Muraoka, H. Nakao, Y. Murakami, H. Sawa, E. Ninomiya, M. Isobe, and Y. Ueda, *Phys. Rev. Lett.* **94**, 106401 (2005).
- ⁷C. Presura, D. van der Marel, A. Damascelli, and R. K. Kremer, *Phys. Rev. B* **61**, 15762 (2000).
- ⁸M. J. Konstantinović, J. Dong, M. E. Ziaei, B. P. Clayman, J. C. Irwin, K. Yakushi, M. Isobe, and Y. Ueda, *Phys. Rev. B* **63**, 121102(R) (2001).
- ⁹H. Smolinski, C. Gros, W. Weber, U. Peuchert, G. Roth, M. Weiden, and C. Geibel, *Phys. Rev. Lett.* **80**, 5164 (1998).
- ¹⁰P. Horsch and F. Mack, *Eur. Phys. J. B* **5**, 367 (1998).
- ¹¹M. Isobe and Y. Ueda, *J. Alloys Compd.* **262–263**, 180 (1997).
- ¹²M. J. Konstantinović, Z. V. Popović, V. V. Moshchalkov, C. Presura, R. Gajić, M. Isobe, and Y. Ueda, *Phys. Rev. B* **65**, 245103 (2002).
- ¹³M. J. Konstantinović, Z. V. Popović, C. Presura, R. Gajić, M. Isobe, Y. Ueda, and V. V. Moshchalkov, *J. Supercond.* **15**, 495 (2002).
- ¹⁴L. Hozoi, S. Nishimoto, and A. Yamasaki, *cond-mat/0501757* (unpublished).
- ¹⁵K. Ohwada, Y. Fujii, N. Takesue, M. Isobe, Y. Ueda, H. Nakao, Y. Wakabayashi, Y. Murakami, K. Ito, Y. Amemiya, H. Fujihisa, K. Aoki, T. Shobu, Y. Noda, and N. Ikeda, *Phys. Rev. Lett.* **87**, 086402 (2001).
- ¹⁶K. Kobayashi, T. Mizokawa, A. Fujimori, M. Isobe, and Y. Ueda, *J. Electron Spectrosc. Relat. Phenom.* **92**, 87 (1998).
- ¹⁷G. A. Sawatzky and D. Post, *Phys. Rev. B* **20**, 1546 (1979).
- ¹⁸S. Shin, S. Suga, M. Taniguchi, M. Fujisawa, H. Kanzaki, A. Fujimori, H. Daimon, Y. Ueda, K. Kosuge, and S. Kachi, *Phys. Rev. B* **41**, 4993 (1990).
- ¹⁹N. S. Hush, *Chem. Phys.* **10**, 361 (1975).
- ²⁰H.-J. Koo and M.-H. Whangbo, *Solid State Commun.* **111**, 353 (1999).
- ²¹K. Siegbahn, C. Nordling, G. Johansson, J. Hedman, P. F. Hedén, K. Hamrin, U. Gelius, T. Bergmark, L. O. Werme, R. Manne, and Y. Baer, *ESCA Applied to Free Molecules* (North-Holland, Amsterdam, 1969).
- ²²A. N. Vasil'ev, V. V. Pryadun, D. I. Khomskii, G. Dhalenne, A. Revcolevschi, M. Isobe, and Y. Ueda, *Phys. Rev. Lett.* **81**, 1949 (1998).
- ²³M. J. Konstantinović, J. C. Irwin, M. Isobe, and Y. Ueda, *Phys. Rev. B* **65**, 012404 (2002).